

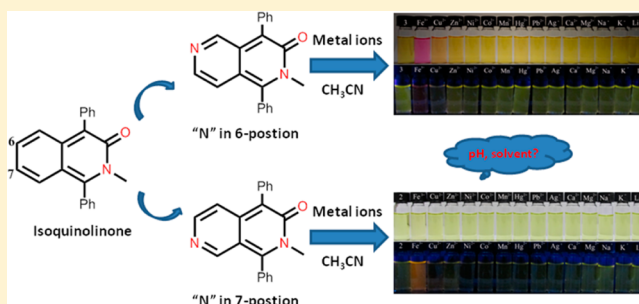
# Azaisoquinolinones: N Positions Tell You Different Stories in Their Optical Properties

Junbo Li, Junkuo Gao, Gang Li, Weiwei Xiong, and Qichun Zhang\*

School of Materials Science and Engineering, Nanyang Technological University, Singapore 639798, Singapore

**S** Supporting Information

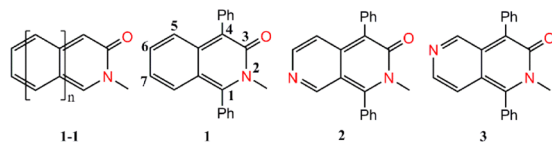
**ABSTRACT:** Since isoquinolinones and their derivatives have been demonstrated to be powerful building blocks in constructing larger acenes and twistacenes, azaisoquinolinones and their analogues could also be important intermediates to approach larger N-heteroacenes. In this paper, we are interested in developing a concise method to synthesize novel azaisoquinolinones building blocks and studying their physical properties. Our results showed that the different N positions have a large effect on the optical and electrochemical properties of azaisoquinolinones. For example, protonation of 6- and 7-azaisoquinolinones shows different shifts of UV-vis and FL spectra. More interestingly, 6- and 7-azaisoquinolinones exhibited different interactions with metal ions in CH<sub>3</sub>CN solution. Upon the addition of 2 equiv of Fe<sup>3+</sup>, 6-azaisoquinolinone displayed an absorption wavelength red-shifted from 470 to 540 nm ( $\Delta\lambda = 70$  nm) with a color change from yellow to red, while the interaction between Fe<sup>3+</sup> and 7-azaisoquinolinone was very weak and there was no obvious color change ( $\Delta\lambda = 18$  nm). Moreover, theoretical calculations confirmed the different optical properties with 6- and 7-azaisoquinolinones.



## INTRODUCTION

Isoquinolinones (Scheme 1) are very attractive not only because they are an important family of biologically relevant

**Scheme 1. Structures of Isoquinolinones (1-1), 2-Methyl-1,4-diphenylisoquinolin-3(2H)-one (1), 7-Aza-2-methyl-1,4-diphenylisoquinolin-3(2H)-one (2), and 6-Aza-2-methyl-1,4-diphenylisoquinolin-3(2H)-one (3)**



alkaloids with key biological activities in the central nervous system<sup>1</sup> but also because they are one type of heteroacene with tunable electronic properties<sup>2</sup> and can act as promising building blocks to construct larger oligoacenes through “clean” reactions.<sup>3</sup> The “clean reaction” strategy is based on thermally eliminating a lactam bridge from precursors to give pure polycyclic compounds through a retro Diels–Alder reaction at high temperature.<sup>3</sup> The attractive factor to employ a “clean” reaction to approach larger acenes is that this method could avoid the tedious purification problem due to the instability and poor solubility of the larger acenes.<sup>4,5</sup> Although N-heteroacenes<sup>6–9</sup> have been demonstrated to be promising materials for ion sensing<sup>8d,f</sup> or as active elements in organic semi-conducting devices such as field effect transistors,<sup>7,9</sup> light-emitting devices,<sup>8i</sup> phototransistors,<sup>8h</sup> memory devices,<sup>8a,b</sup> and

solar cells,<sup>2c</sup> the same dilemma has been encountered in challenging larger N-heteroacenes (more than six linearly fused benzene rings) due to their poor stability, especially the existence of water during the reaction. Thus, a “clean reaction” might be a feasible method to address larger N-heteroacenes. However, in order to realize this strategy, a precursor with build-in heteroatoms is required. Since our previous research has already demonstrated that isoquinolinones and their derivatives are powerful intermediates to prepare larger oligoacenes and twistacenes,<sup>3</sup> we believe that heteroatom (N, P, B)-substituted isoquinolinones and their derivatives should also be promising building blocks to construct larger heteroacenes.

Here, we report the synthesis, characterization, physical properties, and theoretical study of two novel azaisoquinolinones: 7-azaisoquinolinone (2) and 6-azaisoquinolinone (3) (Scheme 1). We found that compounds 2 and 3 have different responses to protonation and metal ions.

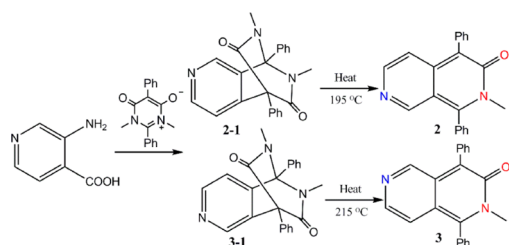
## RESULTS AND DISCUSSION

**Synthesis and Characterization.** 6- and 7-azaisoquinolinones were synthesized in two steps (Scheme 2). The [4 + 2] reaction between 3,4-pyridyne (formed in situ by 3-aminopyridine-4-carboxylic acid and isoamyl nitrite) and mesoionic pyrimidine<sup>10</sup> produced a mixture of isomers 2-1 and 3-1. Fortunately, the isomers can be separated through chromatog-

Received: October 19, 2013

Published: December 3, 2013

## Scheme 2. Synthetic Route to Azaisoquinolinones 2 and 3



raphy. Single crystals of 2-1 were obtained through slowly evaporating a mixed solvent ( $V_{\text{CH}_2\text{Cl}_2}/V_{\text{CH}_3\text{OH}} = 4/1$ ), and the single-crystal structure has been solved for the configuration of 2-1 (Figure 1). Although the precursors 2-1 and 3-1 have

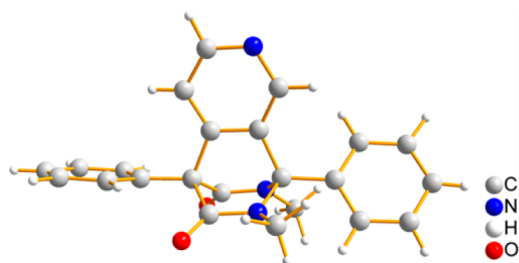


Figure 1. Crystal structure of compound 2-1.

similar structures, the temperatures required to remove the lactam bridge are different (195 °C for compound 2-1 and 215 °C for compound 3-1; Figure S2, Supporting Information). After the removal of the lactam bridge, the target compounds 2 and 3 were obtained. Figure 2 shows the  $^1\text{H}$  NMR spectra of 6-

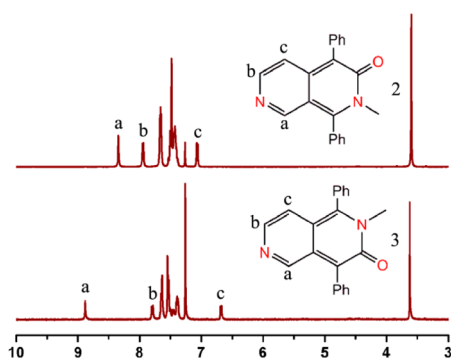


Figure 2.  $^1\text{H}$  NMR spectra of azaisoquinolinones 2 and 3 in  $\text{CDCl}_3$ .

azaisoquinolinone (3) and 7-azaisoquinolinone (2). The most characterized shifts are protons ( $\text{H}_a$ ,  $\text{H}_b$ , and  $\text{H}_c$ ) on the pyridine ring. When the position of the N atom was changed from 7 to 6, the proton  $\text{H}_a$  was shifted downfield from 8.34 to 8.88 ppm. Meanwhile, the protons  $\text{H}_b$  and  $\text{H}_c$  were shifted upfield from 7.94 and 7.96 ppm to 7.79 and 6.68 ppm, respectively. Obviously,  $\text{H}_a$ ,  $\text{H}_b$ , and  $\text{H}_c$  have different chemical environments in compounds 2 and 3. When the position of protons changed from the place near the electron-donating group  $\text{N}-\text{CH}_3$  to the position close to the electron-withdrawing group  $\text{C}=\text{O}$  on the pyridinone ring, the chemical shifts of protons moved downfield accordingly. All new compounds have been fully characterized by  $^1\text{H}$  NMR,  $^{13}\text{C}$  NMR, elemental analysis (EA), and HR-MS.

**Calculations.** Theoretical calculations gave the highest occupied molecular orbital (HOMO) and the lowest unoccupied molecular orbital (LUMO) energy levels of isoquinolinone 1 and azaisoquinolinones 2 and 3 using density functional theory (DFT) at the B3LYP/6-31G\* level.<sup>51</sup> When the 6- or 7-position CH group was substituted by an  $\text{sp}^2$  N atom, both the HOMO and LUMO orbital energy levels were decreased, but the tendencies were different. As shown in Figure 3, the decrease of HOMO orbital energy for

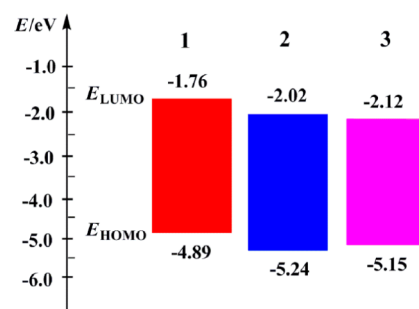


Figure 3. HOMO and LUMO orbital energies calculated by density functional theory (DFT) at the B3LYP/6-31G\* level.

azaisoquinolinone 2 ( $\Delta_{\text{HOMO1-HOMO2}} = 0.35$  eV) is larger than that for azaisoquinolinone 3 ( $\Delta_{\text{HOMO1-HOMO3}} = 0.26$  eV), but the decrease of LUMO orbital energy for azaisoquinolinone 2 ( $\Delta_{\text{LUMO1-LUMO2}} = 0.26$  eV) is smaller than that for 6-azaisoquinolinone 3 ( $\Delta_{\text{LUMO1-LUMO3}} = 0.36$  eV), which induced the band gap of 6-azaisoquinolinone 3 to be smaller than that for 7-azaisoquinolinone (2). Moreover, the HOMO and LUMO orbitals of compounds 1–3 (Figure 4) showed that

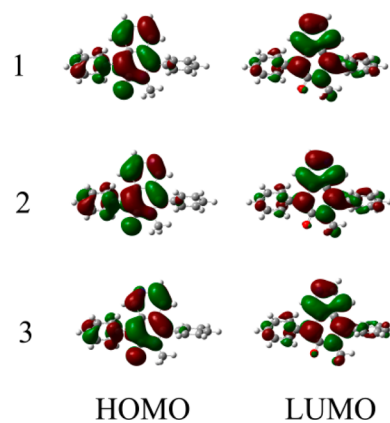
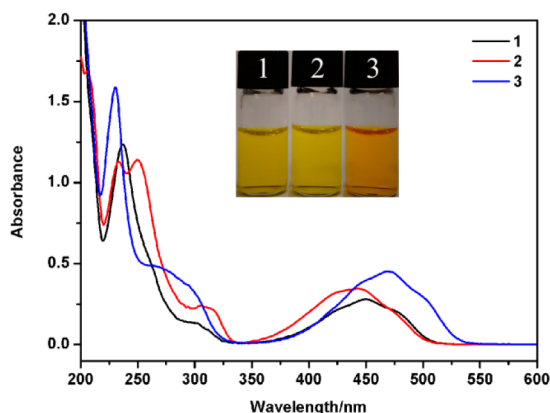


Figure 4. Wave functions for the HOMO and LUMO of compounds 1–3.

the 6-position substitution gives more contribution to the LUMO orbital but the 7-position gives more contribution to the HOMO orbital, which means that 6- and 7-position substitution will strongly affect the bandgap of the related compounds. These interesting theoretical data strongly encouraged us to investigate the differences of 6- and 7-azaisoquinolinones before using them to construct larger N-containing heteroacenes. In addition, since azaisoquinolinones contain N and O atoms, which are well-known atoms for the coordination with metal ions,<sup>12</sup> we believe that azaisoquinolinones should have some responses to metal ions.

**Different Optical and Electrochemical Properties.** The UV–vis absorption and fluorescence spectra of compounds 1–3 were recorded in CH<sub>3</sub>CN at room temperature. As shown in Figure 5, isoquinolinone 1 ( $5 \times 10^{-5}$  M) shows three



**Figure 5.** UV–vis spectra of compounds 1–3 ( $5 \times 10^{-5}$  M) in CH<sub>3</sub>CN. The inset shows the color of compounds 1–3 ( $1 \times 10^{-3}$  M) in CH<sub>3</sub>CN.

absorption bands at 238, 304, and 448 nm. In comparison to compound 1, the two azaisoquinolinones show different shifts. For compound 2, the low-energy region was blue-shifted to 440 nm and the high-energy region was red-shifted to 312 and 251 nm, respectively. For compound 3, in contrast, the low-energy region was red-shifted to 470 nm and the high-energy region was blue-shifted to 272 and 231 nm. The solution containing compound 3 became dark yellow. Moreover, the fluorescence spectra also tell different stories. Compounds 1 and 2 have nearly the same emission maximum wavelengths ( $\lambda_{\text{max}}$  531 nm) and the same intensities, while compound 3 displays a longer emission (544 nm) and a stronger fluorescent intensity in comparison to 1 and 2 (Figure 6). The emission color for

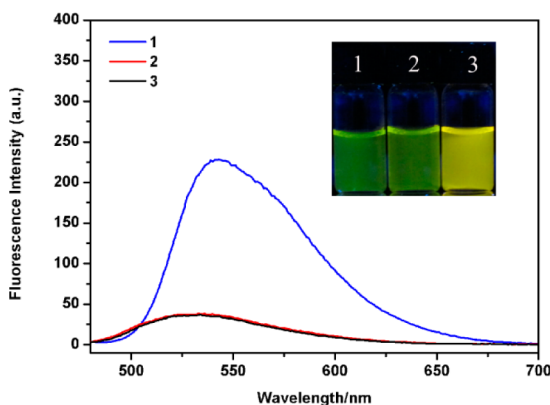


**Figure 6.** Fluorescence spectra ( $1 \times 10^{-5}$  M) of compounds 1–3 in CH<sub>3</sub>CN. The inset shows the fluorescence color of compounds 1–3 ( $1 \times 10^{-3}$  M) in CH<sub>3</sub>CN.

compounds 1 and 2 was green, while it was yellow for compound 3 (Figure 6, inset). Clearly, the UV–vis and FL results suggested that the N positions in azaisoquinolinones have a large effect on their optical responses. Detailed information about the absorption and fluorescence changes for the different azaisoquinolinones can also be obtained from TDDFT (time-dependent DFT) at the B3LYP/6-31G\* level.<sup>11</sup>

The calculated excitation wavelengths of compounds 1–3 are 3.13 eV/445 nm, 3.22 eV/437 nm, and 3.03 eV/458 nm, respectively, which are slightly lower but in good agreement with experiment. Figure S3 (Supporting Information) gives the simulated absorption spectra of compound 1–3. The simulated emission spectra show that the emission wavelengths of compounds 1–3 are at 554, 562, and 580 nm, respectively. The relatively larger red-shift tendency for 7-azaisoquinolinone (3) is in accord with the experimental results (Figure S4, Supporting Information).

The electrochemical properties of compounds 1–3 were studied in a three-electrode electrochemical cell with tetrabutylammonium hexafluorophosphate (Bu<sub>4</sub>NPF<sub>6</sub>, TBAF) (0.1 M) as electrolyte and Ag/AgCl as reference electrode (Figure 7 and Table 1). Compounds 1–3 all show one

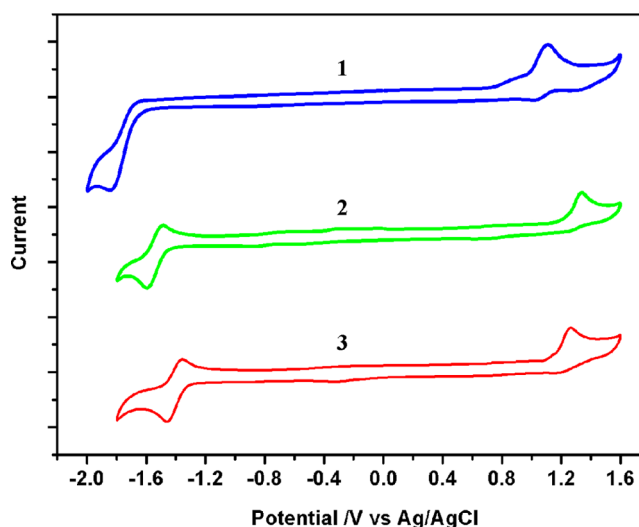


**Figure 7.** Cyclic voltammetry curves of 1–3 in CH<sub>2</sub>Cl<sub>2</sub> solution containing 0.1 M TBAP electrolyte. Scanning rate: 100 mV/s.

irreversible oxidation peak. The onset oxidative potentials for compounds 1–3 were measured as 1.00, 1.25, and 1.18 eV, respectively. On the basis of the equation  $\text{HOMO} = -E_{\text{onset}}^{\text{ox}} - 4.4$  eV,<sup>13</sup> the HOMO energy levels for 1–3 were calculated as  $-5.40$ ,  $-5.65$ , and  $-5.58$  eV, respectively. It is worth noting that the incorporation of an N atom at the 7-position ( $\Delta E_{\text{HOMO}} = -0.25$  eV) induced a larger decrease in HOMO than that at the 6-position ( $\Delta E_{\text{HOMO}} = -0.18$  eV). In addition, compound 1 shows an irreversible reduction peak, while both compounds 2 and 3 show a reversible reduction peak. Their onset reductive potentials were measured as  $-1.67$ ,  $-1.46$ , and  $-1.34$  eV, respectively. The relative LUMO energy levels were calculated as  $-2.73$ ,  $-2.94$ , and  $-3.06$  eV, respectively. Moreover, the decreased value of LUMO for 7-azaisoquinolinone ( $\Delta E_{\text{LUMO}} = -0.21$  eV) is smaller than that for 6-azaisoquinolinone ( $\Delta E_{\text{LUMO}} = -0.33$  eV), which might indicate that compound 3 (6-position) is more stable. The change in tendencies for the HOMO and LUMO is in accord with the calculated results.

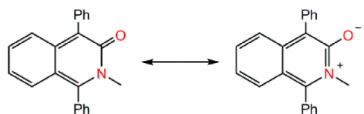
The electronic states of isoquinolinones are strongly governed by its pyridone end unit.<sup>2</sup> There are two possible major contributing resonance structures: one is the neutral polyene state (left), and the other is the charge-separated state (mesoionic state, right) (Scheme 3). Moreover, the electronic state can be readily favored through the choice of solvents. For isoquinolinone 1, in aprotic solvents (CH<sub>2</sub>Cl<sub>2</sub>, THF, DMF,

Table 1. Experimental and Calculated HOMO–LUMO Gaps of Compounds 1–3

compound	$E_{\text{onset}}^{\text{red}}$ (V) <sup>a</sup>	$E_{\text{onset}}^{\text{ox}}$ (V) <sup>a</sup>	$E_{\text{gap}}$ (eV) <sup>b</sup>	LUMO (eV) <sup>c</sup>	HOMO (eV) <sup>d</sup>	$E_{\text{gap}}$ (eV)/ $\lambda_{\text{max}}$ (nm)	LUMO (eV) <sup>f</sup>	HOMO (eV) <sup>f</sup>	$E_{\text{gap}}$ (eV) <sup>f</sup>
1	-1.67	1.00	2.67	-2.73	-5.40	2.77/448	-1.76	-4.89	3.13
2	-1.46	1.25	2.71	-2.94	-5.65	2.82/440	-2.02	-5.24	3.22
3	-1.34	1.18	2.52	-3.06	-5.58	2.64/470	-2.12	-5.15	3.03

<sup>a</sup>Obtained from cyclic voltammograms in  $\text{CH}_2\text{Cl}_2$ . Reference electrode: Ag/AgCl. <sup>b</sup> $E_{\text{gap}} = E_{\text{onset}}^{\text{ox}} - E_{\text{onset}}^{\text{red}}$ . <sup>c</sup>Calculated from cyclic voltammograms. <sup>d</sup>Calculated according to the formula  $E_{\text{HOMO}} = E_{\text{LUMO}} - E_{\text{gap}}$ . <sup>e</sup>Optical band gap,  $E_{\text{gap}} = 1240/\lambda_{\text{max}}$ . <sup>f</sup>Obtained from theoretical calculations.

## Scheme 3. Resonance Structure of Isoquinolinone 1



DMSO), the maximum absorption wavelength is around 448 nm. In protic solvents such as methanol, the maximum absorption peak was blue-shifted to 434 nm, whereas in strongly acidic solvents such as trifluoroacetic acid (TFA), the absorption was blue-shifted to 372 nm (Figure 8a). In relatively weaker acids such as acetic acid, the maximum absorption was at 421 nm, between those for dichloromethane and trifluoroacetic acid. The phenomenon is similar to what we have observed in benzo-fused isoquinolinones.<sup>2</sup>

For azaisoquinolinones 2 and 3, the solvent-induced absorption changes are different. In protic solvent, especially in acidic solvent, there are two equilibria in the system. One is the equilibrium between protonation and deprotonation of the N atom, and another is the resonance between the polyene state and mesoionic state. For 7-azaisoquinolinone (2), the absorption intensity at 440 nm was decreased and blue-shifted to 438 and 434 nm in the  $\text{CH}_3\text{COOH}$  and  $\text{CF}_3\text{COOH}$  solvent systems, respectively. Moreover, a new peak at 334 nm emerged (Figure 8b). Interestingly, the 6-azaisoquinolinone 3 showed different shifts in comparison to 7-azaisoquinolinone 2. In the weakly acidic solvent  $\text{CH}_3\text{COOH}$ , the absorption was blue-shifted from 470 to 458 nm and the onset of the peak reached 600 nm, but in the strongly acidic trifluoroacetic acid, the absorption peak at 470 nm was divided into two peaks at 440 and 500 nm, respectively. The more complicated shifts in azaisoquinolinones are attributed to its greater number of possible resonance structures.

**Optical Responses with Different pHs.** The N atom in azaisoquinolinones should have different responses to the variation of pH values. As shown in Figure 9, the UV–vis and FL spectra changes of compounds 1–3 were investigated in a mixed-solvent system ( $\text{CH}_3\text{CN}/\text{PBS}$  1/1, v/v). Figure 9a,b are the UV–vis and FL spectra of isoquinolinone 1 in different pH solutions. The maximum absorption and emission wavelengths

showed little change within a wide pH span of 1–10. However, for azaisoquinolinones, the protonation of N atoms has a large effect on their optical properties. For 7-azaisoquinolinone 2, when the pH value of the solution was reduced from 10 to 1, the maximum absorption wavelength was red-shifted from 425 to 448 nm ( $\Delta\lambda = 23$  nm) and, accordingly, the emission wavelength was also red-shifted from 531 to 551 nm with increased intensity. Interestingly, when the N position was switched from the 7-position to the 6-position, a larger UV–vis absorption shift from 457 to 515 nm ( $\Delta\lambda = 58$  nm) was observed and the emission wavelength was red-shifted from 544 to 604 nm with some fluorescence quenching. The HOMO and LUMO orbital energies of protonated 6- and 7-azaisoquinolinones (3H, 2H) were calculated using density functional theory (DFT) at the B3LYP/6-31G\* level (Figure S5, Supporting Information). The decrease of LUMO orbital energy with the protonation of 7-azaisoquinolinone 2 is smaller than that of the 6-position N-heteroisoquinolinone 3 ( $\Delta_{\text{LUMO}2\text{-LUMO}2\text{H}} = 4.05$  eV;  $\Delta_{\text{LUMO}3\text{-LUMO}3\text{H}} = 4.32$  eV), but the decreases in values of the HOMO levels are nearly equal ( $\Delta_{\text{HOMO}2\text{-HOMO}2\text{H}} = 3.58$  eV;  $\Delta_{\text{HOMO}3\text{-HOMO}3\text{H}} = 3.62$  eV), which inferred that the band gap of protonated 3 is smaller than that of protonated 2; this could explain why compound 3 has a greater red-shift absorption than 2 during the protonation.

**Optical Responses with Different Metal Ions.** The optical responses of compounds 1–3 with different metal ions were also investigated. Figure 10 shows the UV–vis spectra of 6-azaisoquinolinone 3 upon the addition of 2 equiv of different common metal ions in  $\text{CH}_3\text{CN}$ . As shown in Figure 10, the original color of the solution of 3 is yellow and the maximum absorption wavelength is 470 nm. Upon the addition of 2 equiv of  $\text{Fe}^{3+}$ , the maximum absorption wavelength was largely red-shifted from 470 to 540 nm and the color of the resulting solution changed from yellow to red (Figure 10b). Meanwhile, the addition of other common metal ions such as  $\text{Cu}^{2+}$ ,  $\text{Zn}^{2+}$ ,  $\text{Ni}^{2+}$ ,  $\text{Co}^{2+}$ ,  $\text{Mn}^{2+}$ ,  $\text{Co}^{2+}$ ,  $\text{Pb}^{2+}$ ,  $\text{Ag}^+$ ,  $\text{Ca}^{2+}$ ,  $\text{Mg}^{2+}$ ,  $\text{Na}^+$ ,  $\text{K}^+$ , and  $\text{Li}^+$  has little effect on the UV–vis absorption and there is almost no change in the color of the solutions. These results showed that compound 3 has high selectivity for  $\text{Fe}^{3+}$ . The titration curve showed that, upon the addition of  $\text{Fe}^{3+}$  to a  $\text{CH}_3\text{CN}$  solution of 3, the maximum absorption peak at 470 nm

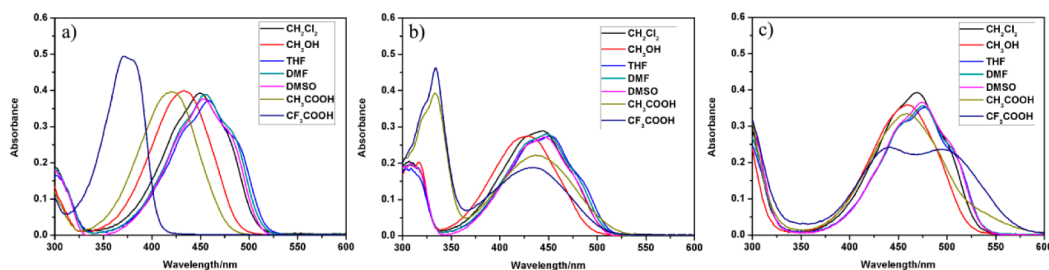
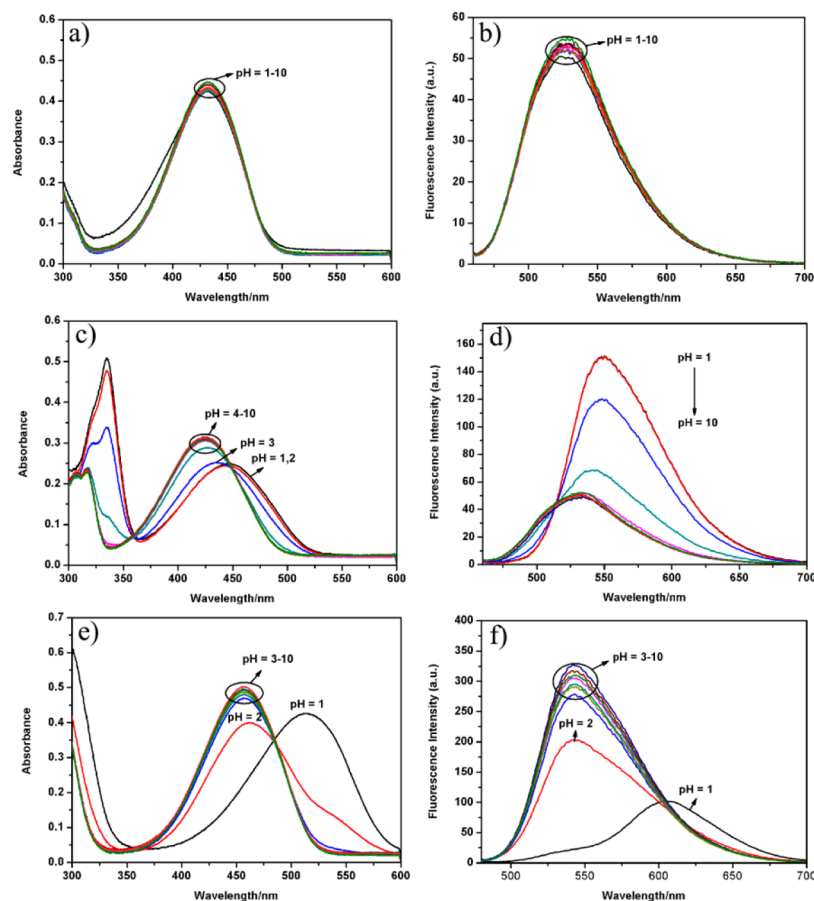
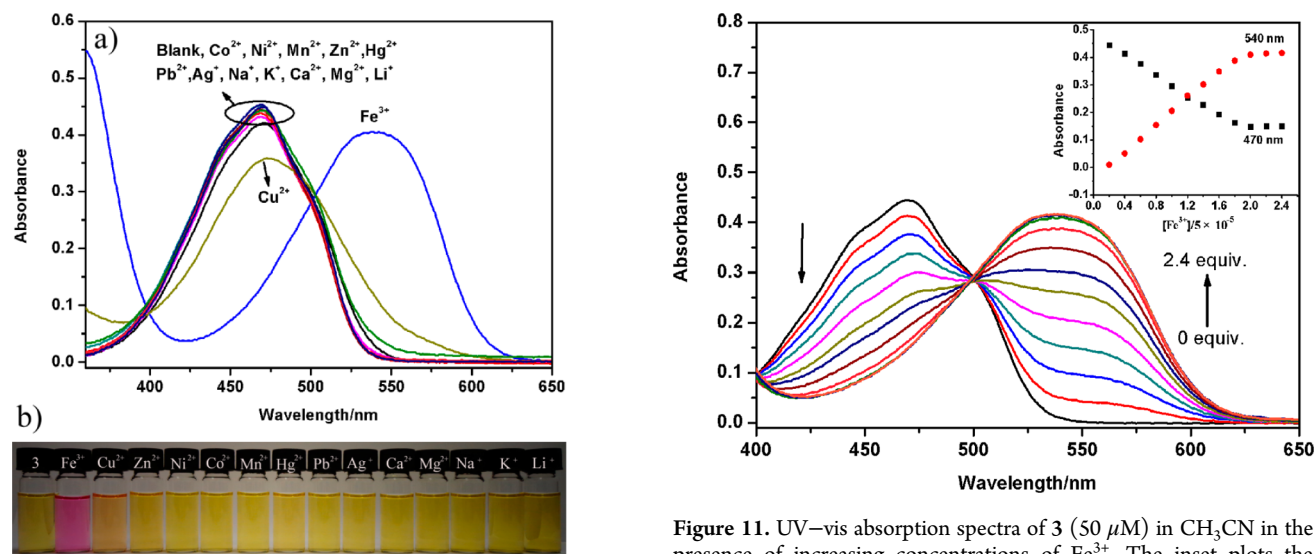


Figure 8. UV–vis absorption spectra of compound 1–3 ( $5 \times 10^{-5}$  M) in different solvents: (a) isoquinolinone 1; (b) 7-azaisoquinolinone 2; (c) 6-azaisoquinolinone 3.



**Figure 9.** UV-vis absorption ( $50 \mu\text{M}$ ) and FL spectra ( $10 \mu\text{M}$ ) of compounds 1–3 at different pH values ( $\text{CH}_3\text{CN}/\text{PBS}$ , 1/1 v/v): (a, b) isoquinolinone 1 (c, d) 7-azaisoquinolinone; (e, f) 6-azaisoquinolinone.



**Figure 10.** (a) UV-vis absorption spectra of 3 ( $50 \mu\text{M}$ ) upon addition of different metal ions (2 equiv) in  $\text{CH}_3\text{CN}$ . (b) Photograph of 3 ( $50 \mu\text{M}$ ) with different metal ions.

decreased while the peak at  $540 \text{ nm}$  increased gradually. The point for the titration to reach saturation is  $\sim 2$  equiv of  $\text{Fe}^{3+}$  (Figure 11). Furthermore, an isosbestic point at  $500 \text{ nm}$  was observed, which indicated the existence of an equilibrium between 3 and the  $3\text{-Fe}^{3+}$  complex.<sup>14</sup> The reversible binding of  $\text{Fe}^{3+}$  was checked using diethylenetriamine or triethylenetetra-

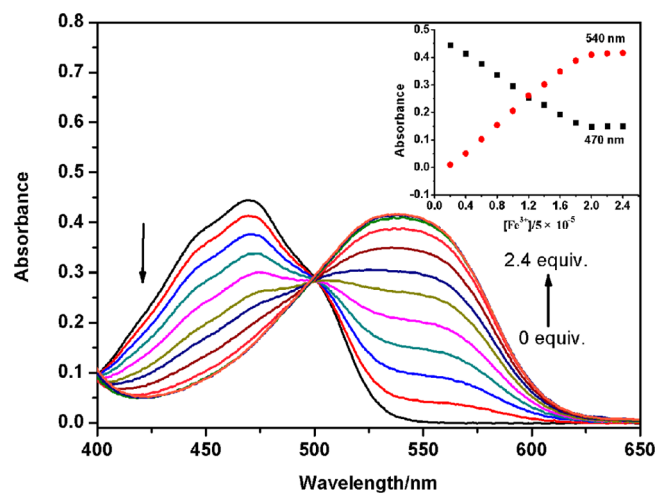


**Figure 11.** UV-vis absorption spectra of 3 ( $50 \mu\text{M}$ ) in  $\text{CH}_3\text{CN}$  in the presence of increasing concentrations of  $\text{Fe}^{3+}$ . The inset plots the absorbance at  $470$  and  $540 \text{ nm}$  versus the  $\text{Fe}^{3+}$  concentration.

amine. First, 2 equiv of  $\text{Fe}^{3+}$  was added to 3, and to this solution was added 2 equiv of diethylenetriamine or triethylenetetramine, which completely restored the original UV-vis and FL spectra of 3 (Figures S6 and S7, Supporting Information).

Job plot data give a 3:2 ratio between 3 and  $\text{Fe}^{3+}$  (Figure 12), which indicated that both the N atom and  $\text{C}=\text{O}$  group might be coordinated with  $\text{Fe}^{3+}$  and a polymer-like complex might be

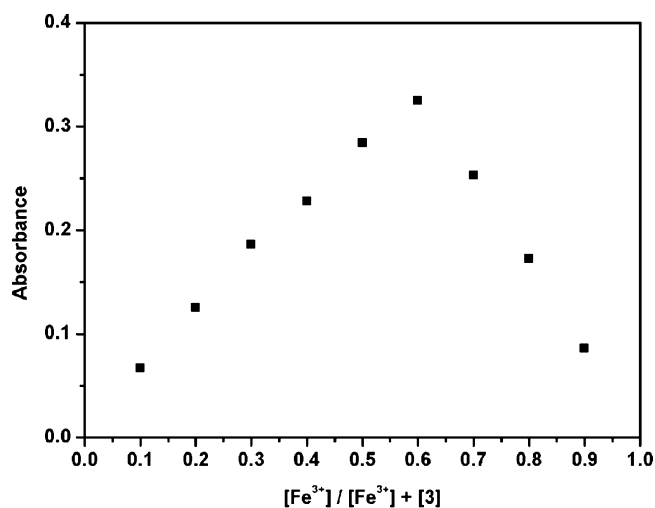


Figure 12. Job plots according to the method of continuous variations. The total concentration of 3 and  $\text{Fe}^{3+}$  is  $10^{-4}$  M.

formed. However, attempts to grow the complex crystal between compound 3 and  $\text{Fe}^{3+}$  were not successful. Meanwhile, upon the addition of  $\text{Fe}^{3+}$ , the UV-vis absorption wavelength of isoquinolinone 1 was blue-shifted (Figure S8, Supporting Information) and the fluorescence was quenched (Figure S9, Supporting Information), which indicated that the  $\text{C}=\text{O}$  group might have some coordination with  $\text{Fe}^{3+}$ . The calculated binding constant of 3 with  $\text{Fe}^{3+}$  is  $1.78 \times 10^6 \text{ M}^{-3/2}$  (Figure S10, Supporting Information). Moreover, the absorbance value at 540 nm was linear with  $\text{Fe}^{3+}$  concentration in the range  $(1-9) \times 10^{-5}$  M. The linear regression equation was determined to be  $A = (4.86 \times 10^3)[\text{Fe}^{3+}] - 0.04$  ( $n = 9$ ,  $R = 0.99805$ ) (Figure 13). The detection limit was calculated to be  $2.5 \times 10^{-7}$  M with

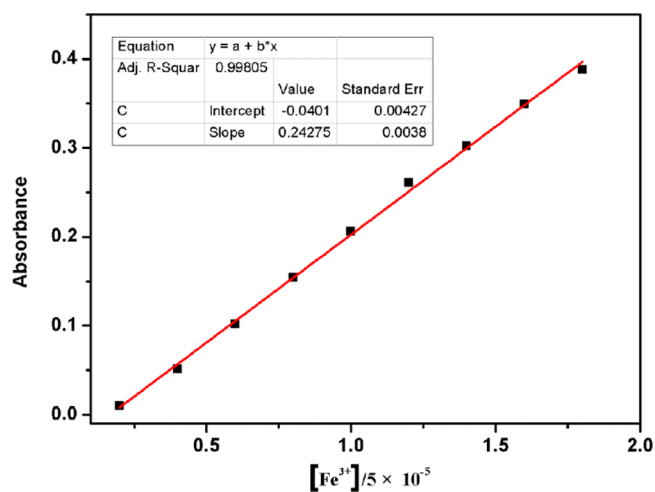


Figure 13. Plot of absorption value at 540 nm versus the concentration of  $\text{Fe}^{3+}$ .

the equation detection limit  $= 3S_d/\rho$ , where  $S_d$  is the standard deviation of blank measurement and  $\rho$  is the slope of the absorbance intensity versus  $\text{Fe}^{3+}$  concentration.<sup>15</sup>

Figure 14 shows the fluorescence spectra of compound 3 ( $10 \mu\text{M}$ ) in  $\text{CH}_3\text{CN}$  upon the addition of different metal ions. On the addition of 2 equiv of  $\text{Fe}^{3+}$  to the solution, the fluorescence of the solution was quenched partially and red-shifted from 554 to 618 nm, while  $\text{Cu}^{2+}$  and  $\text{Ni}^{2+}$  partially quenched the

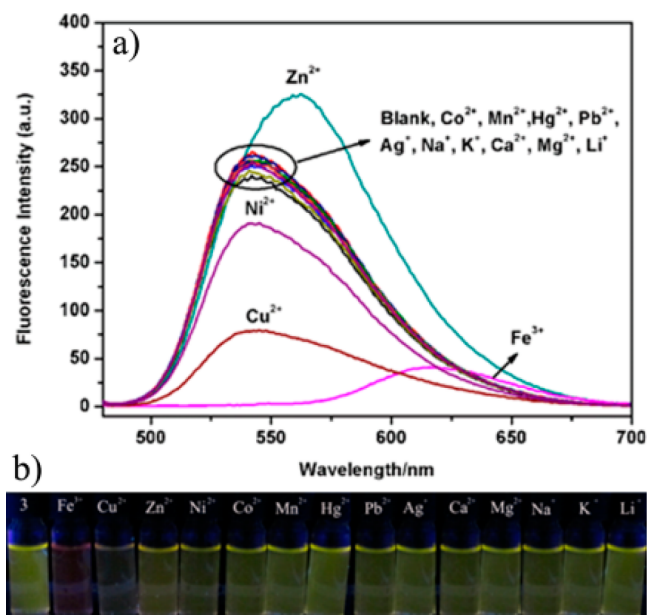


Figure 14. (a) Fluorescence response of 3 ( $10 \mu\text{M}$ ) upon addition of different metal ions (2 equiv) in  $\text{CH}_3\text{CN}$ . (b) Photograph of 3 ( $10 \mu\text{M}$ ) with different metal ions.

fluorescence without a change in the emission wavelength and  $\text{Zn}^{2+}$  led to fluorescence intensity enhancement with the emission wavelength red-shifted to 560 nm. Other metal ions showed little change in emission wavelength and emission intensity. Figure 15 gives the fluorescence response of 3 ( $50 \mu\text{M}$ ) upon addition of different concentrations of  $\text{Fe}^{3+}$ .

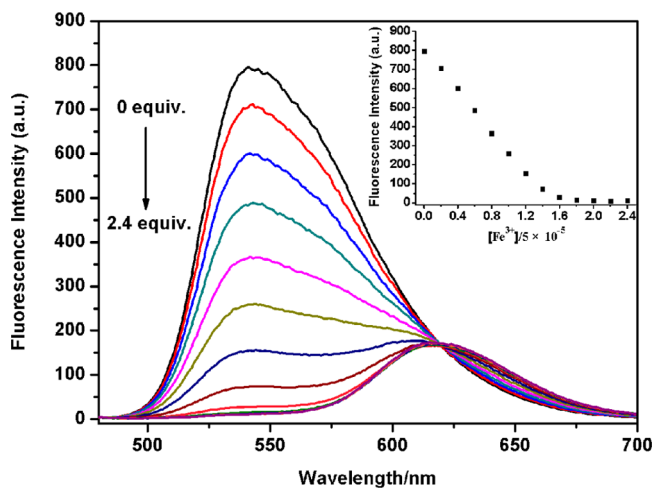
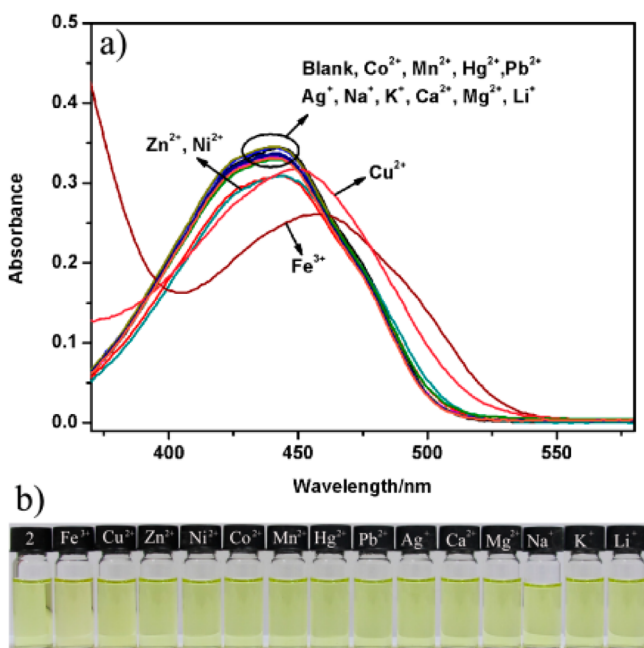


Figure 15. Fluorescence response of 3 ( $50 \mu\text{M}$ ) upon addition of different concentrations of  $\text{Fe}^{3+}$  (2 equiv) in  $\text{CH}_3\text{CN}$ . The inset plots the fluorescence intensity at 554 nm versus  $\text{Fe}^{3+}$  concentration.

Unlike 6-azaisoquinolinone, which could be used as a highly selective colorimetric probe for  $\text{Fe}^{3+}$ , 7-azaisoquinolinone shows a very different optical response to  $\text{Fe}^{3+}$ . Figure 16a shows the UV-vis absorption spectra upon the addition of different metal ions. Obviously, the addition of  $\text{Fe}^{3+}$  induced a smaller red shift ( $\Delta\lambda = 18$  nm) in comparison to that for 6-azaisoquinolinone ( $\Delta\lambda = 70$  nm), while other metal ions only induce a slight shift of the absorption wavelength. A photograph (Figure 16b) shows that the originally light yellow



**Figure 16.** (a) UV-vis absorption spectra of **2** ( $50 \mu\text{M}$ ) upon addition of different metal ions (2 equiv) in  $\text{CH}_3\text{CN}$ . (b) Photograph of **2** ( $50 \mu\text{M}$ ) with different metal ions.

solution ( $5 \times 10^{-5} \text{ M}$ ) was nearly unchanged after the addition of different metal ions, including  $\text{Fe}^{3+}$ . The fluorescence change seems more interesting. Unlike the case for compound **3**, which shows partial fluorescence quenching and a red shift upon the addition of  $\text{Fe}^{3+}$ , the fluorescence intensity of compound **2** was enhanced while the emission wavelength was also red-shifted from 531 to 555 nm. Figure 17b shows that the emission color changes from blue to orange after the addition of 2 equiv of  $\text{Fe}^{3+}$ .

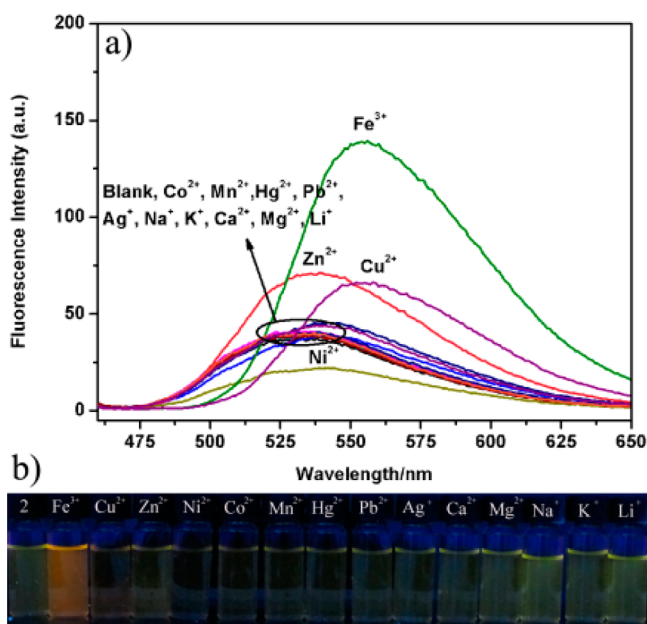


**Figure 17.** (a) Fluorescence response of **2** ( $10 \mu\text{M}$ ) upon addition of different metal ions (2 equiv) in  $\text{CH}_3\text{CN}$ . (b) Photograph of **2** ( $10 \mu\text{M}$ ) with different metal ions.

## CONCLUSIONS

In summary, we have synthesized and fully characterized two novel azaisoquinolinones: 6- and 7-azaisoquinolinone. Theoretical calculations and electrochemical results showed that the N atom at the 6-position of the isoquinolinone structure had a greater contribution to the LUMO, while 7-position substitution contributes more to the HOMO. Our research showed that the 6-azaisoquinolinone exhibited a larger red shift in UV absorption and fluorescence in comparison to 7-azaisoquinolinone during protonation. More interestingly, 6-azaisoquinolinone can be used as a colorimetric probe for  $\text{Fe}^{3+}$ , while the 7-azaisoquinolinone did not show any color change. All the above results clearly demonstrated that the N-substituted positions have a great effect on the optical properties. Future work in our group will focus on using the 6- and 7-azaisoquinolinones as building blocks to construct larger N-containing heteroacenes and trying to understand how N-positions affect the properties of targeted N-heteroacenes.

## EXPERIMENTAL SECTION

**General Procedure.** The stock solutions (10 mM) of chloride salts of  $\text{Fe}^{3+}$ ,  $\text{Cu}^{2+}$ ,  $\text{Zn}^{2+}$ ,  $\text{Ni}^{2+}$ ,  $\text{Co}^{2+}$ ,  $\text{Hg}^{2+}$ ,  $\text{Ca}^{2+}$ ,  $\text{Mg}^{2+}$ ,  $\text{Na}^+$ ,  $\text{K}^+$ , and  $\text{Li}^+$  and nitrate salts of  $\text{Pb}^{2+}$ ,  $\text{Mn}^{2+}$ , and  $\text{Ag}^+$  were prepared in deionized water. Stock solutions (1 mM) of compounds **1–3** were prepared in acetonitrile.

**Optical Study.** A 3.0 mL portion of acetonitrile solvent was placed in a quartz cell (10.0 mm width), and  $150 \mu\text{L}$  (for UV-vis) or  $30 \mu\text{L}$  (for FL) of compounds **1–3** was added. To these solutions was added  $30 \mu\text{L}$  (for UV-vis) or  $6 \mu\text{L}$  (for FL) of metal ions. For all measurements, the excitation wavelength was at 450 nm for **1** and **2**, and 470 nm for **3**. The slit width for both excitation and emission was 5.0 nm.

**Synthesis. Compound 2-1.** Under an atmosphere of dry argon, mesoionic pyrimidine **3** (2 g, 6.83 mmol) and excess isoamyl nitrite (6 mL) were added to 150 mL of 1,2-dichloroethane. The mixture was heated to reflux, and then 3-aminopyridine-4-carboxylic acid (1.14 g, 8.26 mmol) dispersed in 50 mL of 1,2-dichloroethane was added to the mixture dropwise. After addition, the mixture was refluxed for 12 h. Then, the mixture was cooled to room temperature and the solvent was removed under reduced pressure. The resultant residue was purified by silica gel column chromatography using  $\text{CH}_2\text{Cl}_2/\text{CH}_3\text{OH}$  (100/1, v/v) as eluent to afford compound **2-1** as a white solid (630 mg, 25%). Mp: decomposition at  $195^\circ\text{C}$ . IR (KBr,  $\text{cm}^{-1}$ ):  $\nu$  3035, 2958, 1716, 1675, 1581, 1477, 1414, 1375, 1206, 1010, 756, 704.  $^1\text{H}$  NMR ( $\text{CDCl}_3$ , 300 MHz):  $\delta$  2.72 (s, 6H), 6.87 (d, 1H,  $J = 6 \text{ Hz}$ ), 7.47–7.53 (m, 3H), 7.66–7.70 (m, 3H), 7.86 (d, 2H,  $J = 6 \text{ Hz}$ ), 8.13 (d, 2H,  $J = 6 \text{ Hz}$ ), 8.46 (d, 1H,  $J = 6 \text{ Hz}$ ), 8.75 (s, 1H).  $^{13}\text{C}$  NMR ( $\text{CDCl}_3$ , 75 MHz):  $\delta$  34.2, 66.5, 80.1, 120.8, 127.8, 128.3, 129.4, 130.1, 130.5, 130.6, 131.4, 135.9, 141.6, 148.1, 149.7, 171.0. HR-MS:  $[\text{M} + \text{H}]^+$  calcd 370.1556, found 370.1554. Anal. Calcd for  $\text{C}_{23}\text{H}_{19}\text{N}_3\text{O}_2$ : C, 74.78; H, 5.18; N, 11.37. Found: C, 74.56; H, 5.02; N, 11.56.

**Compound 3-1.** The same procedure was used as for the synthesis of **2-1**: white solid, yield 20%. Mp: decomposition at  $215^\circ\text{C}$ . IR (KBr,  $\text{cm}^{-1}$ ):  $\nu$  3053, 2943, 1716, 1677, 1583, 1452, 1414, 1379, 1196, 1087, 1006, 833, 753, 698.  $^1\text{H}$  NMR ( $\text{CDCl}_3$ , 300 MHz):  $\delta$  2.69 (s, 6H), 7.46–7.56 (m, 4H), 7.64–7.72 (m, 3H), 7.80–7.83 (m, 2H), 8.12 (s, 1H), 8.17–8.19 (m, 2H), 8.59 (d, 1H,  $J = 6 \text{ Hz}$ ).  $^{13}\text{C}$  NMR ( $\text{CDCl}_3$ , 75 MHz):  $\delta$  34.1, 64.6, 80.3, 115.9, 127.8, 128.3, 129.4, 130.1, 130.3, 130.5, 130.6, 131.3, 133.9, 147.0, 148.4, 148.9, 171.4. HR-MS:  $[\text{M} + \text{H}]^+$  calcd 370.1556, found 370.1554. Anal. Calcd for  $\text{C}_{23}\text{H}_{19}\text{N}_3\text{O}_2$ : C, 74.78; H, 5.18; N, 11.37. Found: C, 74.62; H, 5.12; N, 11.46.

**7-Aza-2-methyl-1,4-diphenylisoquinolin-3(2H)-one (2).** A neat sample of compound **2-1** (300 mg, 0.81 mmol) was purged three times using nitrogen before heating at  $195^\circ\text{C}$  under vacuum for 6 h to give a yellow solid (250 mg, nearly 100%). Mp:  $251\text{--}253^\circ\text{C}$ . IR (KBr,  $\text{cm}^{-1}$ ):  $\nu$  3056, 1629, 1609, 1532, 1440, 1294, 1024, 817, 758, 706.  $^1\text{H}$  NMR ( $\text{CDCl}_3$ , 300 MHz):  $\delta$  3.60 (s, 3H), 7.07 (d, 1H,  $J = 6 \text{ Hz}$ ),

7.40–7.51 (m, 7H), 7.65–7.67 (m, 3H), 7.95 (d, 1H,  $J = 6$  Hz), 8.34 (s, 1H).  $^{13}\text{C}$  NMR ( $\text{CDCl}_3$ , 75 MHz):  $\delta$  36.2, 113.5, 115.2, 118.8, 127.7, 128.5, 128.9, 129.5, 130.6, 130.8, 131.3, 134.4, 139.2, 144.8, 155.2, 155.3, 160.2. MALDI-TOF:  $[M + H]^+$  calcd 313.1341, found 313.1340. Anal. Calcd for  $\text{C}_{21}\text{H}_{16}\text{N}_2\text{O}$ : C, 80.75; H, 5.16; N, 8.97. Found: C, 80.70; H, 5.02; N, 8.79.

**6-Aza-2-methyl-1,4-diphenylisoquinolin-3(2H)-one (3).** A neat sample of compound **3-1** (300 mg, 0.81 mmol) was purged three times using nitrogen before heating at 215 °C under vacuum for 6 h to give a red solid (240 mg, nearly 100%). Mp: 202–204 °C. IR (KBr,  $\text{cm}^{-1}$ ):  $\nu$  3056, 1627, 1604, 1520, 1436, 1371, 1292, 1024, 750, 700.  $^1\text{H}$  NMR ( $\text{CDCl}_3$ , 300 MHz):  $\delta$  3.63 (s, 3H), 6.58 (d, 1H,  $J = 6$  Hz), 7.38–7.46 (m, 3H), 7.52–7.55 (m, 4H), 7.63–7.65 (m, 3H), 7.79 (d, 1H,  $J = 6$  Hz), 8.88 (s, 1H).  $^{13}\text{C}$  NMR ( $\text{CDCl}_3$ , 75 MHz):  $\delta$  36.7, 116.4, 118.1, 122.9, 128.2, 128.5, 129.0, 129.5, 130.3, 131.1, 132.2, 133.5, 132.5, 137.1, 150.4, 151.8, 160.5. HR-MS:  $[M + H]^+$  calcd 313.1341, found 313.1340. Anal. Calcd for  $\text{C}_{21}\text{H}_{16}\text{N}_2\text{O}$ : C, 80.75; H, 5.16; N, 8.97. Found: C, 80.67; H, 5.10; N, 8.86.

## ■ ASSOCIATED CONTENT

### ■ Supporting Information

Figures, a table, and CIF files giving crystal data of **2-1**, simulated UV–vis and FL spectra, and original FTIR,  $^1\text{H}$  NMR,  $^{13}\text{C}$  NMR, and HR-MS spectra. This material is available free of charge via the Internet at <http://pubs.acs.org>.

## ■ AUTHOR INFORMATION

### Corresponding Author

\*E-mail for Q.Z.: [qczhang@ntu.edu.sg](mailto:qczhang@ntu.edu.sg).

### Notes

The authors declare no competing financial interest.

## ■ ACKNOWLEDGMENTS

Q.Z. acknowledges financial support from AcRF Tier 1 (RG 16/12) and Tier 2 (ARC 20/12 and ARC 2/13) from the MOE and the CREATE program (Nanomaterials for Energy and Water Management) from the NRF.

## ■ REFERENCES

- (1) (a) Shamma, M. *The Isoquinoline Alkaloids*. Chemistry and Pharmacology; Academic Press: New York, 1972. (b) Shamma, M.; Moniot, J. L. *Isoquinolinone Alkaloid Research*; Plenum Press: New York, London, 1978. (c) Müjded, B.; Özcan, S.; Balci, M. *Phytochem. Lett.* **2011**, *4*, 407. (d) Nakano, H.; Hongo, H. *Heterocycles* **1993**, *51*, 37. (e) Fukumi, H.; Kurihara, H. *Heterocycles* **1978**, *9*, 1197.
- (2) (a) Craig, I. M.; Duong, H.-M.; Wudl, F.; Schwartz, B. J. *Chem. Phys. Lett.* **2009**, *477*, 319. (b) Li, G.; Duong, H.-M.; Zhang, Z.-H.; Xiao, J.-C.; Liu, L.; Zhao, Y.-L.; Zhang, H.; Huo, H.-W.; Li, S.-Z.; Ma, J.; Wudl, F.; Zhang, Q. *Chem. Commun.* **2012**, *48*, 5974. (c) Zhang, Q.; Xiao, J.-C.; Yin, Z.-Y.; Duong, H.-M.; Qiao, F.; Boey, F.; Hu, X.-A.; Zhang, H.; Wudl, F. *Chem. Asian J.* **2011**, *6*, 856. (d) Zhang, Q.; Divayana, Y.; Xiao, J.-C.; Wang, Z.-J.; Tiekink, E. R. T.; Doung, H.-M.; Zhang, H.; Boey, F.; Sun, X.-W.; Wudl, F. *Chem. Eur. J.* **2010**, *16*, 7422.
- (3) (a) Xiao, J.-C.; Malliakas, C.-D.; Liu, Y.; Zhou, F.; Li, G.; Su, H.-B.; Kanatzidis, M.-G.; Wudl, F. *Chem. Asian J.* **2012**, *7*, 672. (b) Xiao, J.-C.; Liu, S.-W.; Liu, Y.; Ji, L.; Liu, X.-W.; Zhang, H.; Sun, X.-W.; Zhang, Q. *Chem. Asian J.* **2012**, *7*, 561. (c) Xiao, J.-C.; Duong, H.-M.; Liu, Y.; Shi, W.-X.; Ji, L.; Li, G.; Li, S.-Z.; Liu, X.-W.; Ma, J.; Wudl, F.; Zhang, Q. *Angew. Chem., Int. Ed.* **2012**, *51*, 6094. (d) Xiao, J.-C.; Divayana, Y.; Zhang, Q.; Doung, H.-M.; Zhang, H.; Boey, F.; Sun, X.-W.; Wudl, F. *J. Mater. Chem.* **2010**, *20*, 8167. (e) Li, J.-B.; Zhang, Q. *Synlett* **2013**, *24*, 686.
- (4) (a) Bailey, W.; Liao, C. W. *J. Am. Chem. Soc.* **1955**, *77*, 992. (b) Fang, T. *Heptacene, Octacene, Nonacene, supercene and related polymers*; Ph.D. Dissertation, University of California, Los Angeles, CA, 1986. (c) Momndal, R.; Shah, B. K.; Neckers, D. C. *J. Am. Chem.*

*Soc.* **2006**, *128*, 9612. (d) Bettinger, H. F.; Mondal, R.; Neckers, D. C. *Chem. Commun.* **2007**, 5209. (e) Momndal, R.; Tönshoff, C.; Khon, D.; Neckers, D. C. *J. Am. Chem. Soc.* **2009**, *131*, 14281. (f) Kaur, I.; Stein, N. N.; Kopreski, R. P.; Miller, G. P. *J. Am. Chem. Soc.* **2009**, *131*, 3424. (g) Kaur, I.; Jazdzzyk, M.; Stein, N. N.; Prusevich, P.; Miller, G. P. *J. Am. Chem. Soc.* **2010**, *132*, 1261. (h) Tönshoff, C.; Bettinger, H. F. *Angew. Chem., Int. Ed.* **2010**, *49*, 4125.

(5) (a) Ferguson, G.; Parvez, M. *Acta Crystallogr., Sect. B: Struct. Crystallogr. Cryst. Chem.* **1979**, *35*, 2419. (b) Duong, H. M.; Bendikov, M.; Steiger, D.; Zhang, Q.; Sonmez, G.; Yamada, J.; Wudl, F. *Org. Lett.* **2003**, *5*, 4433. (c) Payne, M. M.; Parkin, S. R.; Anthony, J. E. *J. Am. Chem. Soc.* **2005**, *127*, 8028. (d) Chun, D.; Cheng, Y.; Wudl, F. *Angew. Chem., Int. Ed.* **2008**, *47*, 8380. (e) Purushothaman, B.; Bruzek, M.; Parkin, S. R.; Miller, A. F.; Anthony, J. E. *Angew. Chem., Int. Ed.* **2011**, *50*, 7013.

(6) (a) Bunz, U. H. F.; Engelhart, J. U.; Linder, B. D.; Schafforth, M. *Angew. Chem., Int. Ed.* **2013**, *52*, 3810. (b) Lindner, B. D.; Engelhart, J. U.; Tverskoy, O.; Appleton, A. L.; Rominger, F.; Peters, A.; Himmel, H. J.; Bunz, U. H. F. *Angew. Chem., Int. Ed.* **2011**, *50*, 8588. (c) Tverskov, O.; Rominger, F.; Peters, A.; Himmel, H. J.; Bunz, U. H. F. *Angew. Chem., Int. Ed.* **2011**, *50*, 3557. (d) Bunz, U. H. F. *Pure Appl. Chem.* **2010**, *82*, 953. (e) Bunz, U. H. F. *Chem. Eur. J.* **2009**, *15*, 6780. (f) Appleton, A. L.; Brombosz, S. M.; Barlow, S.; Sears, J. S.; Bredas, J. L.; Marder, S. R.; Bunz, U. H. F. *Nat. Commun.* **2010**, *1*, 91.

(7) (a) Maio, Q. *Synlett* **2012**, 326. (b) Liu, D. Q.; Xu, X. M.; Su, Y. R.; He, Z. K.; Xu, J. B.; Miao, Q. *Angew. Chem., Int. Ed.* **2013**, *52*, 6222. (c) Miao, Q.; Nguyen, T. Q.; Someya, T.; Blanchet, G. B.; Nuckolls, C. *J. Am. Chem. Soc.* **2003**, *125*, 10284. (d) Liang, Z. X.; Tang, Q.; Mao, R. X.; Liu, D. Q.; Xu, J. B.; Miao, Q. *Adv. Mater.* **2011**, *23*, 5514. (e) Liang, Z. X.; Tang, Q.; Xu, J. B.; Miao, Q. *Adv. Mater.* **2011**, *23*, 1535. (f) Tang, Q.; Liang, Z. X.; Liu, J.; Xu, J. B.; Miao, Q. *Chem. Commun.* **2010**, *46*, 2977.

(8) (a) Gu, P. Y.; Zhou, F.; Gao, J.; Li, G.; Wang, C.; Xu, Q. F.; Zhang, Q.; Lu, J.-M. *J. Am. Chem. Soc.* **2013**, *135*, 14086. (b) Li, G.; Zheng, K.; Wang, C.; Leck, K. S.; Hu, F.; Sun, X. W.; Zhang, Q. *ACS Appl. Mater. Interfaces* **2013**, *5*, 6458. (c) Li, G.; Long, G.; Chen, W.; Hu, F.; Chen, Y.; Zhang, Q. *Asian J. Org. Chem.* **2013**, *2*, 852. (d) Li, G.; Wu, Y. C.; Gao, J. K.; Li, J. B.; Zhao, Y.; Zhang, Q. *Chem. Asian J.* **2013**, *8*, 1574. (e) Zhao, J.; Wong, J. I.; Wang, C.; Gao, J.; Ng, V. Z. Y.; Yang, H. Y.; Loo, S. C. J.; Zhang, Q. *Chem. Asian J.* **2013**, *8*, 665. (f) Zhao, J.-F.; Li, G.; Wang, C.-Y.; Chen, W.-Q.; Chye, S.; Loo, J.; Zhang, Q.-C. *RSC Adv.* **2013**, *3*, 9653. (g) Li, G.; Wu, Y. C.; Gao, J. K.; Wang, C. Y.; Li, J. B.; Zhang, H. C.; Zhao, Y.; Zhao, Y. L.; Zhang, Q. *J. Am. Chem. Soc.* **2012**, *134*, 20298. (h) Wu, Y. C.; Yin, Z. Y.; Xiao, J. C.; Liu, Y.; Wei, F. X.; Tan, K. J.; Kloc, C.; Huang, L.; Yan, Q. Y.; Hu, F. Z.; Zhang, H.; Zhang, Q. *ACS Appl. Mater. Interfaces* **2012**, *4*, 1883. (i) Li, G.; Putu, A. A.; Gao, J. K.; Divayana, Y.; Chen, W. Q.; Zhao, Y.; Sun, X. W.; Zhang, Q. *Chem. Asian J.* **2012**, *1*, 346.

(9) (a) Liu, Y. Y.; Song, C. L.; Zeng, W. J.; Zhou, K. G.; Shi, Z. F.; Ma, C. B.; Yang, F.; Zhang, H. L.; Gong, X. *J. Am. Chem. Soc.* **2010**, *132*, 16349. (b) Smith, J. C.; Ma, K.; Piers, W. E.; Parvez, M.; McDonald, R. *Dalton Trans.* **2010**, *39*, 10256.

(10) Kappe, T.; Pocivalnik, D. *Heterocycles* **1983**, *20*, 1367.

(11) (a) Hehre, W. J.; Ditchfie, R.; Pople, J. A. *J. Chem. Phys.* **1972**, *56*, 2257. (b) Becke, A. D. *J. Chem. Phys.* **1993**, *98*, 5648.

(12) (a) He, X. R.; Liu, H. B.; Li, Y. L.; Wang, S.; Li, Y. J.; Wang, N.; Xiao, J. C.; Xu, X. H.; Zhu, D. B. *Adv. Mater.* **2005**, *17*, 2811. (b) Li, J.-B.; Hu, Q.-H.; Yu, X.-L.; Zeng, Y.; Cao, C.-C.; Liu, X. W.; Guo, J.; Pan, Z.-Q. *J. Fluoresc.* **2011**, *21*, 2005. (c) Li, J.-B.; Yu, X.-L.; Liu, X.-W.; Gao, Y.; Zeng, Y.; Hu, Q.-H.; Pan, Z.-Q. *Sensor Lett.* **2011**, *9*, 1331.

(13) (a) Hong, W.; Yuan, H.; Li, H.; Yang, X.; Gao, X.; Zhu, D. *Org. Lett.* **2011**, *13*, 1410. (b) Jiang, Z. Q.; Zhang, W. J.; Yao, H. Q.; Yang, C. L.; Cao, Y.; Qin, J.; Yu, G.; Liu, Y. *J. Polym. Sci., Part A: Polym. Chem.* **2009**, *47*, 3651.

(14) (a) Kumari, N.; Jha, S.; Bhattacharya, S. *J. Org. Chem.* **2011**, *76*, 8215. (b) Zhu, M.; Yuan, M. J.; Liu, X. F.; Xu, J. L.; Lv, J.; Huang, C. S.; Liu, H. B.; Li, Y. L.; Wang, S.; Zhu, D. B. *Org. Lett.* **2008**, *10*, 1481. (c) Yuan, M. J.; Zhou, W. D.; Liu, X. F.; Zhu, M.; Li, J. B.; Yin, X. D.;



Zheng, H. Y.; Zuo, Z. C.; Ouyang, C. B.; Liu, H. B.; Li, Y. L.; Zhu, D. B. *J. Org. Chem.* **2008**, *73*, 5008.  
(15) Yuan, M. J.; Li, Y. L.; Li, J. B.; Li, C. H.; Liu, X. F.; Lv, J.; Xu, J. L.; Liu, H. B.; Wang, S.; Zhu, D. B. *Org. Lett.* **2007**, *9*, 2313.